Magnetospheric Driving of Saturn's Thermosphere during Storm-Like Events

Nicholas Achilleos[1], Christopher G. A. Smith[2] & Alan D. Aylward[1]
[1]Department of Physics and Astronomy, University College London; [2]UCL Visiting Fellow, Department of Physics and Astronomy

Download Poster: www.ucl.ac.uk/~ucapnac/posters/nach agu2010 poster.pdf

Abstract

Observations of Saturn's aurora have provided compelling evidence that the main oval is coincident with the boundary between open and closed magnetic flux, and that the surface area interior to this oval can change dramatically during strong episodes of magnetic reconnection ('substorms') in the magnetotail region. We show results of numerical experiments using the UCL axisymmetric model of Saturn's thermosphere (Smith et al., 2005) which reveal the following aspects thermospheric flow during such events:

1. The enormous inertia of the thermosphere introduces a delay of order 1 planetary day between the peak magnetospheric and peak thermospheric angular velocities.
2. This delay results in a period where thermospheric rotation exceeds magnetospheric, and the corresponding field-aligned currents transfer angular momentum from the magnetosphere to atmosphere, rather than the reverse situation which pertains in the steady state.
3. The thermospheric inertia also leads to flow speeds significantly more rapid (>10%) than the steady state, up to several planetary days after storm subsidence.

Introduction

There is compelling evidence, from correlation of *in situ* solar wind data from *Cassini* and auroral images from Hubble Space Telescope (HST) (e.g. Bunce et al. (2006); Badman et al. (2005)), that the solar wind conditions control the level of Saturn's auroral precipitation, in a picture where the oval represents an Earth-like 'polar cap boundary' between closed and open magnetic flux (e.g. Cowley et al. (2005)).

Theoretical work (Cowley et al., 2005; Badman et al., 2005) interprets the large poleward excursions of auroral emission observed at Saturn, following strong magnetospheric compressions, as hot magnetospheric electrons precipitating into the atmosphere after magnetotail reconnection, leading to closure of significant levels (tens of GWb) of open flux.

From an atmospheric viewpoint, such an event would affect slowly rotating thermospheric gas, poleward of northern oval latitudes $\sim 75°$. Neutrals in this region would be driven, during a reconnection event, through collisions with ionospheric plasma with angular velocity in the range between observed 'polar cap' values of $\sim 0.3\Omega_S$ (Stallard et al., 2004) ('open flux' conditions; pre-reconnection) and $\sim 0.8\Omega_S$ (typical values in outer, closed magnetosphere; post-reconnection). Here Ω_S is the planetary angular velocity, which we have taken to be $1.6236 \times 10^{-4} s^{-1}$ (period 10.75 hr).

Here we show results of a 'numerical experiment' where the magnetospheric angular velocity (Ω_M) profile, used to drive the UCL 2-D Saturn Thermosphere Model, has been varied in both time and latitude. The Figures show the results of this semi-qualitative simulation of a reconnection event, in terms of its effect on neutral and magnetospheric dynamics and energy flow. The model has time-dependent values of both (i) latitude of the polar cap boundary; and (ii) Ω_M value in the 'active region' between the latitudes of the cap boundary under quiet conditions and under 'maximum storm' conditions (most contracted cap). This time-dependence for both features is assumed to be proportional to a simple, analytic 'storm function' which implements change on the time scale of $\tau_S =\sim 0.4$ planetary days - in future studies we will further refine this value, using available observations.

Results

Atmospheric Dynamics and Aurora

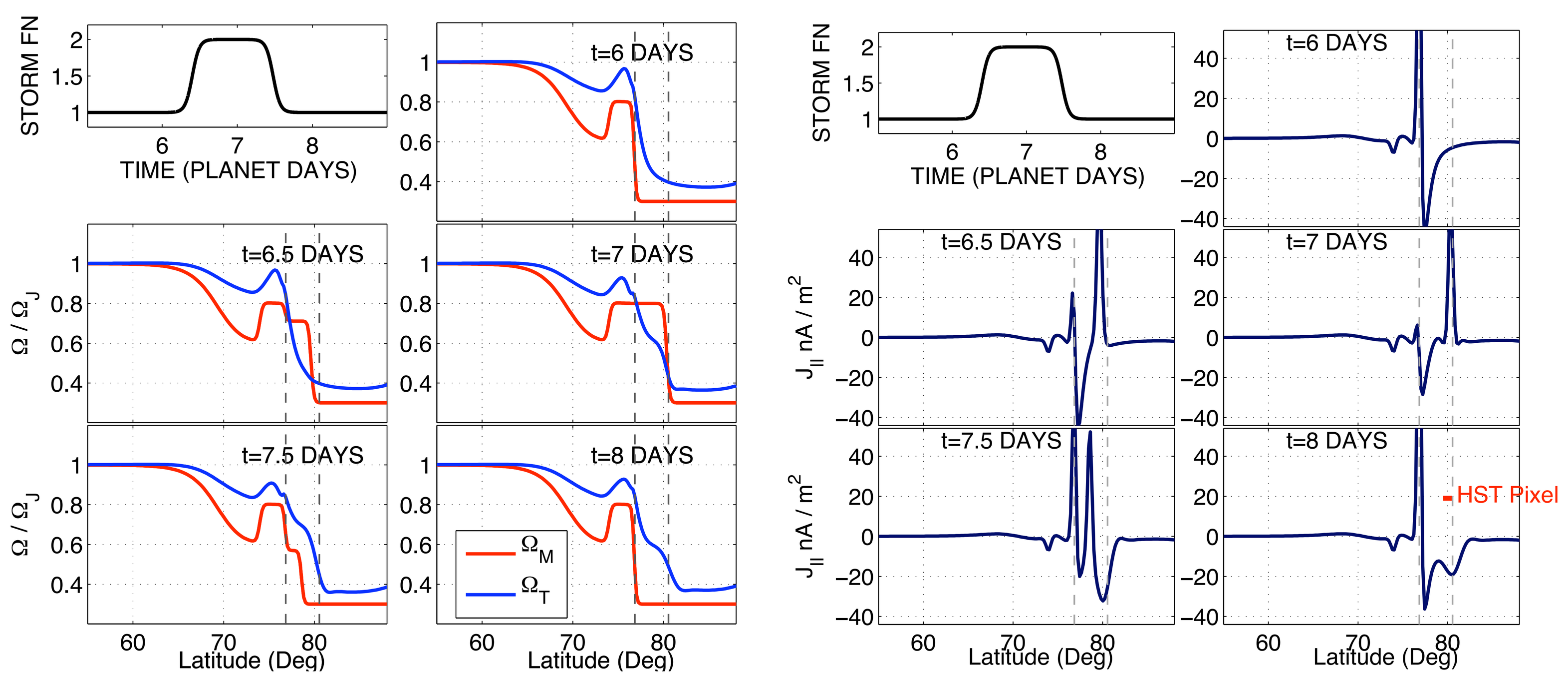

FIGURE 1: The left-hand set of plots shows the angular velocities of the magnetosphere (Ω_M, coloured red) and thermosphere (Ω_T, coloured blue) during the simulation, as a function of time. The 'storm function' indicates the qualitative 'phase' of the storm event, and controls the changes in the polar cap boundary location and magnetospheric Ω_M in the 'active region' (latitudes 75–$80°$). Ω_T is a weighted average over the pressure levels in the model, which corresponds to an equatorward Pedersen current J_θ proportional to $(\Omega_T - \Omega_M)$. The quiescent system (T=6 days) before the event shows the expected steady-state behaviour $\Omega_M < \Omega_T$ at all latitudes. At T=6.5 days ('ascending phase'), Ω_M in the active region has increased above Ω_T – the thermosphere's enormous inertia prevents Ω_T from responding instantly to this imposed Ω_M, thus we see a reversal in the usual ordering, i.e. $\Omega_M > \Omega_T$.

This reversal persists at the 'peak phase', T=7 days, where we see evidence of the delayed response of the thermosphere (increased Ω_T). The 'descending phase', T=7.5 days, sees the restoration of the steady-state ordering, although the profiles are quite disturbed compared to the quiescent phase. Finally, the 'post-storm' phase, T=8 days (0.5 days after storm subsides), shows the system returning to its quiescent state – although clear differences in active region Ω_T are still apparent.

The right-hand plots show the corresponding auroral (field-aligned) current profiles at each phase of the event. The change in Ω_M and Ω_T profiles produces a rich variety of auroral forms, some of which would correspond to observations of multiple auroral arcs. The angular size of an HST ACS pixel is shown for comparison.

Joule Heating

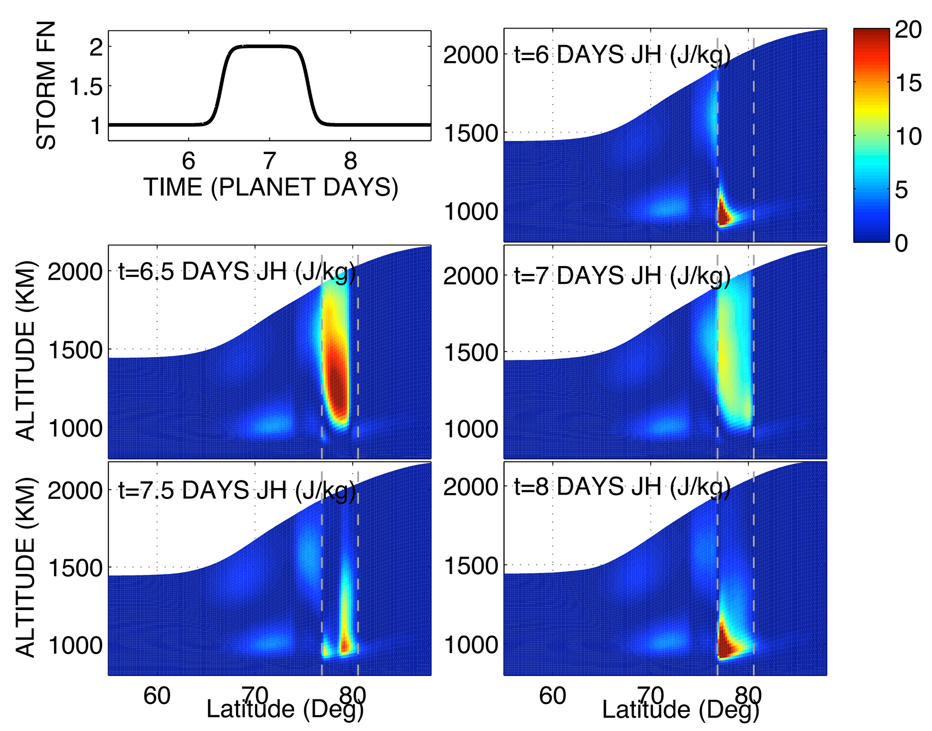

FIGURE 2: The colour scale indicates Joule heating predicted by the model as a function of latitude and altitude above the 1-Bar pressure level. The quiescent phase shows the maximum corresponding to the auroral ionization peak near $\sim 76°$, 1000 km. The other phases show a great variety of heating profiles corresponding to the rotation and auroral current profiles shown in Figure 1.

Temperature

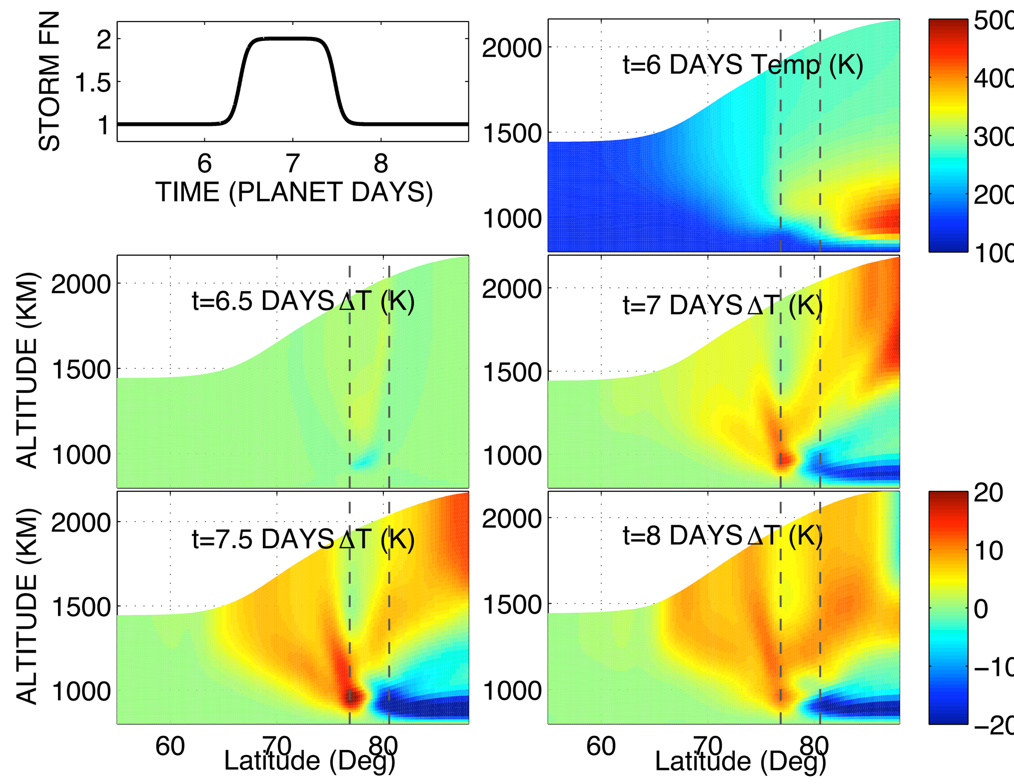

FIGURE 3: The colour scale indicates temperature in the thermosphere as a function of latitude and altitude; active region boundaries are shown by vertical dashed lines. For the quiescent phase (t=6 days), total temperature of the neutrals is indicated – the increased temperature in the polar cap region is produced by advection of heat energy from the auroral region (see the Joule heating distribution in Figure 2). The other phases show temperature *differences* relative to quiescent. Widespread fluctuations in temperature are transported by winds from the auroral regions, both poleward and equatorward of the active region. Temperature fluctuations up to ~ 20K are evident in the high-altitude polar cap region. Cooling is also evident near the lower boundary of the polar cap region, associated with strong upwelling. A future study will examine in more detail the correlation between atmospheric flows and these global patterns of temperature.

References

Badman S. V., Bunce E. J., Clarke J. T., Cowley S. W. H., Gérard J., Grodent D., Milan S. E., 2005, J. Geophys. Res., 110, A11216

Bunce E. J., Cowley S. W. H., Jackman C. M., Clarke J. T., Crary F. J., Dougherty M. K., 2006, Advances in Space Research, 38, 806

Cowley S. W. H., Badman S. V., Bunce E. J., Clarke J. T., Gérard J., Grodent D., Jackman C. M., Milan S. E., Yeoman T. K., 2005, J. Geophys. Res., 110, A02201

Smith C. G. A., Aylward A. D., Miller S., Müller-Wodarg I. C. F., 2005, Ann. Geophys., 23, 2465

Stallard T. S., Miller S., Trafton L. M., Geballe T. R., Joseph R. D., 2004, Icarus, 167, 204